Annu. Rev. Phys. Chem. 2004. 55:559–83
doi: 10.1146/annurev.physchem.55.091602.094156

First published online as a Review in Advance on February 3, 2004

AMORPHOUS WATER

C. Austen Angell
Department of Chemistry and Biochemistry, Arizona State University, Tempe, Arizona 85287-1604; email: CAA@asu.edu

Key Words HDA, LDA, VHDA, ideal glass, boson peak, cryoelectron microscopy, polyamorphism, hyperquench, glass transition

■ **Abstract** After providing some background material to establish the interest content of this subject, we summarize the many different ways in which water can be prepared in the amorphous state, making clear that there seems to be more than one distinct amorphous state to be considered. We then give some space to structural and spectroscopic characterization of the distinct states, recognizing that whereas there seems to be unambiguously two distinct states, there may be in fact be more, the additional states mimicking the structures of the higher-density crystalline polymorphs. The low-frequency vibrational properties of the amorphous solid states are then examined in some detail because of the gathering evidence that glassy water, while difficult to form directly from the liquid like other glasses, may have some unusual and almost ideal glassy features, manifested by unusually low states of disorder. This notion is pursued in the following section dealing with thermodynamic and relaxational properties, where the uniquely low excess entropy of the vitreous state of water is confirmed by three different estimates. The fact that the most nearly ideal glass known has no properly established glass transition temperature is highlighted, using known dielectric loss data for amorphous solid water (ASW) and relevant molecular glasses. Finally, the polyamorphism of glassy water, and the kinetic aspects of transformation from one form to the other, are reviewed.

1. INTRODUCTION

This review is not as broad at the title suggests. Ordinary water and supercooled water are both amorphous states of water (the stable and principal metastable states) and both are very mature subjects with extensive literatures. In a 1983 review of supercooled water in this journal (1), I noted just how old that subject was, the first review having appeared in 1775. It is clear that a full review of this subject would be unmanageable. Thus, we limit our objectives to the solid form of amorphous water. This is a much more recent subject of attention and, to the best of my knowledge, it has not so far been the sole subject of a review since the classic chapter of Sceats & Rice (2).

The idea that there is an amorphous solid form of water was first put forward in 1935 when Burton & Oliver (3, 3a) deposited water molecules onto a cold plate and

showed that the X-ray diffraction pattern that characterized the deposit lacked any Bragg peaks. The question of whether this material is to be regarded as a vitreous material or only as the more ambiguous form of matter known as "amorphous solid," is one of the matters this review addresses. I hope to provide readers with the basis for making their own decisions on this matter. First, I give some reasons for being more than passingly interested in this noncrystalline solid state of water.

Amorphous solid water is, to start, a very abundant material, galactically speaking. It is reputed to be the most abundant form of water in the universe, thanks to its propensity for forming, molecule by molecule, as a deposit on interstellar dust particles (3–4a). There is a large astrophysical literature on amorphous solid water (ASW), much of it dealing with reactions occurring in or on amorphous water or with gas-solid relationships relevant to comet behavior. These issues are beyond the scope of this review.

Further to its importance in this respect, amorphous water is no ordinary amorphous solid. When it is subject to increasing pressure, it first softens and then quite suddenly collapses to a denser but still amorphous form (5–7). This behavior is also seen in computer simulation studies of water, in which the density and structure of the high-density form depends on the particular potential function chosen to represent the water (8–9) and, to a lesser extent, on the temperature of the simulation. On release of pressure, what is observed depends on the temperature of observation. At 76 K the density remains at the new higher value, but above about 110 K the amorphous form recovers its original larger volume by an equally abrupt process (5–7). This surprising behavior has awakened a great deal of interest in the concept of vitreous polymorphs (10, 10a), or what has now become known as polyamorphism (11–13).

Finally, it is becoming increasingly clear that low-density amorphous water (LDA), among glassy solids, is of extraordinary character. Despite the noncrystalline nature of the molecular arrangements, both the thermodynamic state and the vibrational characteristics are those of a highly ordered substance. The heat-carrying phonons of low-temperature amorphous water behave like those in a crystal, with a mean free path that increases with decreasing temperature. No other glass shows this behavior. It seems likely that in low-density amorphous water we closely approach the ideal glass state. These characteristics will be dealt with in some detail in this review, Sections 4.1.2 and 4.3.

Similar but less dramatic behavior has been observed in a succession of other tetrahedrally coordinated amorphous solids, studied by both laboratory (14–17) and computer simulation (8, 8a, 20–20b) methods. Most of this group of compounds (SiO_2, GeO_2, $ZnCl_2$, etc.) are unambiguously glassy because they can be formed from the liquid during slow cooling and can consequently exhibit glass transitions during reheating. Whether or not amorphous water confirms its glassiness by exhibiting a glass transition is very much a matter of debate at this time, as discussed in Section 4.

In Section 2, this review first examines the different routes by which amorphous water in its different forms has been prepared, without more than cursory consideration of the properties of the products. This necessarily involves some

structural characterization, which is dealt with in more detail in Section 3. Section 4 describes the properties of amorphous water in its different manifestations and considers whether amorphous water is properly described as glassy or vitreous and what its glass transition temperature might be. Finally, Section 5 examines in more depth the phenomenon of polyamorphism in water.

2. FORMATION

While the original preparation of ASW (3) utilized the vapor deposition process, essentially the same material has now been made by a number of quite different routes (5–7, 46–48b). Furthermore, by using the same route, and changing only the conditions of deposition, a distinct and different amorphous water of much higher density has been made (2, 4). The different routes used for amorphous water formation are a subset of those that have been used to form more conventional glassy solids (21, 21a), and a modified version of figure 1 of Reference 21 could be used to depict them. Here we merely list them, giving representative, not exhaustive, examples of the preparations and the studies in which they have been used.

Vapor deposition methods were used to prepare samples of ASW by many workers for the following physical studies:

a. For calorimetry: Ghormley (22), McMillan & Los (23), Sugisaki et al. (24), McFarlane & Angell (25), Johari et al. (26), and Hallbrucker et al. (27–27b);
b. For spectroscopy: Buentempo (28), Rice and coworkers (29–30), and Yoshimura & Kanno (31);
c. For vapor pressure and free energy studies: Speedy et al. (32);
d. For crystallization studies: Skripov and coworkers (33), Jennsikens & Blake (35), Schmitt et al. (34), Kay and coworkers (36);
e. For dielectric relaxation studies: Korveda et al. (35, 37), and Johari et al. (37a);
f. For neutron and X-ray diffraction structure studies: Wenzel et al. (38) and Narten et al. (39);
g. For diffusion studies: Scott & Kay (40) and Smith et al. (40a) and ion penetration (nano-viscosity) studies: Tsekouras et al. (41);
h. For electron microscope studies of vitrification: Dubochet & Lepault (42) and many who followed this work;
i. For vibrational dynamics studies by neutron scattering: Kolesnikov et al. (43) and Yamamuro et al. (44);
j. For thermal conductivity studies: Andersson & Suga (45).

A closely related method is the trapping on a cold plate the aqueous product of appropriate vapor-phase chemical reactions, the so-called chemical vapor deposition method, but this has not been reported.

Water has been vitrified directly from the liquid by *liquid hyperquenching* of micron-sized droplets produced in different ways or by hyperquenching thin films

a. Directly into a cryofluid by Brügeller & Mayer (46, 46a), Dubochet & McDowell (47), and many subsequent cryo-electronmicroscopists (see below);
b. Onto cold plates by Mayer (48–48b) and Small and coworkers (49, 49a).

Recently, it was claimed that it is possible to produce thick glassy water at moderate quench rates by injection of water into a diamond wedge or onto a diamond wafer (50). However, it is unlikely that this method actually produced glassy water. This is because the transparent material obtained did not yield a sharp crystallization exotherm at temperatures a little above the weak effect attributed to the glass transition at 135 K. The sharp crystallization exotherm commencing in the range of 150–160 K during reheating is the one universal feature of all previous studies of ASW or vitreous water. However, transparent, but highly crystallized, samples are the rule for reheated glassy aqueous solutions near the water-rich glass-forming limit (10, 10a). All that is required to understand this notion is that the crystals form ubiquitously by homogeneous nucleation and remain ungrown (hence below the wavelength of light).

Because the formation of glassy water by this method [hyperquenched glassy water (HQG)] is more technical, fewer studies have been made and they are mainly the work of one group (51–51e). A range of thermodynamic, spectroscopic, and crystallization studies have been reported (51–51e), and after appropriate annealing, the properties of the two forms, ASW and HQG, seem almost indistinguishable. Recently others have begun to exploit this technique for different spectroscopic purposes (49, 49a).

A less rapid quench is required (52), or a thicker vitreous sample can be obtained (53–53b), if the liquid being quenched is under very high pressure (52–53b) and is subdivided. For instance, Mishima & Suzuki (52) have vitrified water by rapidly cooling emulsified water between indium gaskets in a low–thermal mass assembly from which heat is extracted via liquid nitrogen–cooled anvils that grip the sample assembly. The pressures acting on the sample are estimated to be at least 0.2 gigaPascals (Gpa) and probably about 0.5 GPa, and the quenching rate is about 10^{3° K s^{-1} (52). Mishima & Suzuki showed that the structure of the phase obtained was "roughly resembling" high-density amorphous (HDA) water, which had previously been obtained only by nonliquid routes. Sartori et al. (53) showed that for a given cooling rate the thickness of sample that can be vitrified can be increased tenfold by high-pressure quenching.

The HDA phase of water can thus be obtained in several ways. The first preparation was by vapor deposition at 10 K by Rice and coworkers (2, 38), who did not clarify completely the conditions that predetermine the form of amorphous water that is obtained. Astrophysicists now believe that the high-density form is always the form obtained by very low–temperature vapor deposition, that is, at temperatures below 30 K in thin films (3). This is the condition under which most

amorphous water is formed in interstellar space, so it should be the high-density form of amorphous water that is the most abundant form of water in the universe. When prepared in the most familiar way, discussed next, this high-density form is called HDA. However, this acronym should probably not yet be applied to the high-density form obtained by vapor deposition or pressure quenching because all HDA waters seem to be somewhat different depending on the method and conditions of preparation (56).

The best-known method of obtaining the high-density form is that pioneered by Mishima et al. (5–7; 56; see also reviews in Reference 12) in which ordinary crystalline ice is subjected to pressures in excess of 1.6 GPa at liquid nitrogen temperature and collapses to the amorphous state. This is called "pressure-induced amorphization." There is currently a lot of discussion about the actual density of the most stable form of HDA ice, because the densities that have been reported are very variable (5, 39). The density depends on the temperature of formation, mode of formation, and whether the formation involves spinodal collapse (54–55) of the crystal or nucleation and growth of the new phase. Some others who have explored this mode of preparation are Floriano et al. (56–56b) for structure studies; Mishima & Suzuki (57) for phase transition studies; Johari (58c) for density and penetrometry measurements and glass temperature studies; Klug and coworkers (59, 61) for calorimetry, phase transformation, and spectroscopy studies; Schober and coworkers (62–64) for neutron scattering studies of vibrational dynamics and HDA–low-density amorphous (LDA) phase transition kinetics; Brazhkin and coworkers for phase transition kinetics (65, 65a); Kolesnikov et al. (43) and Yamamuro et al. (44) for vibrational dynamics; and Finney et al. (44a) for neutron diffraction studies of structure. The precise relation between the forms of HDA waters made by Mishima's two methods and the earlier methods developed by electron microscopists (52b,c) is not yet clear, though the discussion by Dubochet and colleagues (67) is helpful in this connection.

A modification of the mechanically induced vitrification method that requires no high pressure apparatus is the *cold microtoming method* described by Dubochet and coworkers (68). These workers have shown that when ice is microtomed the combination of shear stress and local pressure is sufficient to produce the amorphous state. The state obtained is similar to HDA water produced at very high pressure (about 1 GPa) from hexagonal ice and annealed close to its transformation temperature of 117 K. This type of vitreous water is evidently not suitable for high-resolution electron microscopy of embedded tissue or biomolecules. [When the embedding medium is formed around the molecule or tissue of interest in an unstressed manner, for example, by fast quenching of the aqueous medium to avoid ice crystals, then the embedded molecules, tissues, etc. find themselves in a structureless medium that proves ideal for structural study by electron microscopy. This electron microscopy technique, cryoEM, pioneered by Dubochet (69), is now the subject of enormous activity, first reviewed in Reference 70. It made possible the determination of the 3D structure of ribosome (71). The embedding medium is universally referred to as "vitreous ice" by this community (70–72)].

In contrast to the pressure-induced amorphization method, ASW can be obtained by *decompression amorphization*. First described in Reference 73, and in more detail in Reference 55, this has now been put into practice by by Tulk & Klug (74) using ice XII as the starting high-pressure phase.

While the microtoming procedure referred to above is a sort of mechanical damage–induced vitrification, there have been no demonstrations yet that simple ball-milling can vitrify ice, as is demonstrated frequently for other glass formers (75, 75a). However, both *electron bombardment vitrification* (67, 76, 76a) and *radiation damage–induced vitrification* of water have been reported (77, 77a). For amorphization of different crystal forms by irradiation, the dose needed is comparable, but it must be delivered at lower temperatures, the more stable the crystalline phase being amorphized (67).

The question of whether amorphous water can be produced in more or less pure form by *phase-separation vitrification* from supercooled aqueous solutions (12) (in the way that pure SiO_2 droplets can be observed to separate from alkali silicate solutions of appropriate composition during annealing) is still undecided.

While the vitrification of water by laboratory methods poses some problems, particularly when undertaken by the liquid route, it is very simple, indeed almost unavoidable, to vitrify the liquid in *computer simulation vitrification*, using molecular dynamics. Here the slowest available cooling is usually unable to permit crystallization, though crystallization has recently been achieved by holding systems for long periods at the optimum temperature (78, 79). Without these special efforts, the simulated liquid undergoes "ergodicity-breaking" (i.e., falling out of equilibrium) with all the aspects of the glass transition phenomenon expected from laboratory studies of glass-forming substances (80). Usually the strong upswing in heat capacity seen in bulk laboratory supercooling water (81) is missing because the pair potentials in use do not lead to a condensed phase with the same high degree of cooperativity that real water exhibits; that is, the strong increase in heat capacity in the liquid state (81) is mostly missing or rather weak. The change in heat capacity observed (80, 82) is then more or less the difference between ordinary water and ice. This is nevertheless a large change in heat capacity, indeed about 15 times the value reported by experimentalists at the putative glass temperature of 135 K (26, 59). As seen below, the nature and position in temperature of the glass transition for amorphous water is at the center of a major controversy.

3. STRUCTURE

The first question that is usually asked about a vitreous material concerns the difference between its structure and those of its crystalline analogs. In the case of vapor-deposited ASW, the answer depends, as indicated above, on the conditions of formation.

In the earliest detailed study of this question, Wenzel et al. (38) showed that the deposit obtained by deposition at liquid N_2 temperature was ice I–like in structure. The random open network character of ASW was shortly confirmed in the X-ray

study of Narten et al. (39). The most interesting aspect of the latter study was the finding that there was a second form of ASW in which an additional peak at 3.3 Å occurred. This was interpreted as due to water molecules included interstitially in the random network to achieve a higher density. This result was obtained for a sample deposited at low temperature (10 K) and was the first indication that there could be structural polyamorphs of water. Rice and coworkers (2, 29a, 30b, 39), particularly Narten et al. (39), clearly anticipated that there could be amorphous forms of all or many of the different crystalline ice polyamorphs, though it could not be known without additional measurements that these forms could coexist in metastable equilibrium, as has since been suggested by the studies of Mishima (5–7, 57) and others (63).

There have since been many X-ray (57), electron-scattering (84), and neutron-scattering (3, 44, 57, 85–90) studies of HDA water obtained by pressure amorphization and LDA derived from it. HDA water has a density of 1.17 g cm^{-3} (90) compared with water at its density maximum, 1.00 g cm^{-3}, and LDA water (obtained by decompression and warming to 120 K), 0.94 g cm^{-3} (90). Floriano et al. (90) suggested that the HDA structure was that of the glass that would be obtained by isobaric vitrification of water at 1.0 GPa. It is interesting in this respect that on reheating at ambient pressure, HDA water starts to relax from its as-formed state as low as 87 K (61, 64, 91) and then transforms to LDA in the range of 98–103 K. This is to be contrasted with the behavior of the HDA form obtained (52) by quenching the liquid at lower pressures (0.2–0.5 GPa), which only transforms to LDA at the higher temperature of 130 K. (52). The latter thus appears to be the more stable form.

Dubochet and coworkers (67) discussed the differences in electron diffraction patterns obtained for hyperquenched glassy water ("plunge-frozen") (67), high pressure vitrified water, and the amorphous product of irradiation amorphization of ice III or IX (no distinction being possible between these two polymorphs by their methods). The structure of the amorphous form obtained by irradiation of the high-pressure crystal proves to be indistinguishable from that obtained by high-pressure liquid vitrification but is clearly different from that of the lower-density HQG (based on diffuse diffraction ring diameter). Each is presumably close to the structure of HDA water at the point of transformation back to LDA on decompression at 100 K (see Section 5). The density of ices III and IX is about 1.16 g cm^{-3} (cf. the value attributed to HDA above).

The differences in structure between these different high-density forms is of course of interest. Mishima attempted to determine the structure of the liquid-quenched form of HDA using a combination of X-ray diffraction and Raman scattering, but the spectra were not of good quality, leading to the description "rough resemblance" to the HDA structure mentioned above (52).

It is presumably significant that HDA water produced by cold compression to 1.8 GPa is capable (93, 94) of nucleating the unusual ice polymorph ice XII (95), which is the first example of a four-connected net containing only seven- and eight-membered rings (96). The density of ice XII, however (1.4365 g cm^{-3}) (95), is significantly higher than that of HDA water at pressure, reported by Mishima

et al. (97) to be 1.31 g cm^{-3}, so the structures will be only in the same topological class rather than one being a disordered version of the other.

Finney et al. (44a), reminiscent of Narten et al. (39), regard the structure of HDA water as differing from that of LDA water mainly by the presence of a fifth nearest neighbor interstitial, which causes the radial order to decrease while the spatial order increases (so that HDA water resembles ordinary liquid water), a somewhat different density picture from that offered originally by Floriano et al. (90). The interstitial water molecule plays the role of a lynch pin (44a) in the stabilization of the HDA structure. There is no room, according to this analysis (44a), for microcrystalline interpretations (55, 58b) of the structure of HDA water. The similarity of densities of HDA water and ice III and the fact that a structure indistinguishable from that of high pressure–quenched vitreous water forms on electron irradiation of cold ice III (67) strongly suggest a randomized form of ice III as a good description of HDA water. This structure differs from LDA water not in hydrogen bond distances but in the manner in which a fifth neighbor is incorporated in the first coordination shell.

A larger value of the ambient pressure density of HDA water, 1.299 g cm^{-3}, has been given recently by Johari (98), which highlights the fact that the density of the high-pressure phases of vitreous ice is quite variable.

The recent reports (99) of an ambient pressure amorphous ice with high density [1.25 $\pm$ 0.41 g cm^{-3}; higher than that given by Floriano et al. (90) and Mishima et al. (97) but less than the value given by Johari (98)] have been given a lot of attention (44a). [There is a new acronym, VHDA (99). This phase (very HDA)] is tentatively distinguished from HDA by the reproducibility of its density when prepared in the same manner, for example, holding a sample of HDA water under compression while raising the temperature to 165 K, then dropping the temperature to 77 K and removing the pressure. The initial implication has been that this should be a new and distinct polyamorph, as indeed would be supported from the recent computer simulation work of Brovchenko et al. (102). The latter authors, using restricted ensemble Monte Carlo simulations, have given evidence for the possible existence of multiple liquid-liquid transitions, as discussed in more detail in Section 5. Tentative structural interpretations for VHDA water (44a) have leaned toward a model in which there is double occupancy of interstitial sites within the hydrogen-bonded network.

This is an interesting area in which much more activity may be expected. It is an area where there may be difficulty distinguishing, by laboratory studies, between a sample that has been found at low-lying level in a distinct configuration space megabasin (in a configuration space that allows density as an additional dimension) (104) and a sample trapped kinetically at different levels in the same megabasin. In the former case the escape (from the megabasin characteristic of one phase to the megabasin characteristic of the other) should require a nucleation event (21a, 104) [unless the temperature is very low when it must occur by a spinodal collapse (54, 54a)]. In the latter case, that is, within a single megabasin, annealing to lower energies should be continuous but may become extremely slow.

4. PROPERTIES OF AMORPHOUS WATERS

4.1. Vibrational Dynamics

4.1.1. HIGH-FREQUENCY MODES The vibrational dynamics of amorphous water in its different manifestations have been widely researched (2, 28, 30, 31, 61, 82, 91, 105–107). The highest-frequency fundamental internal modes of the water molecule are manifested in the infra red at $\sim$3000 cm^{-1} for the $-$OH stretch when the hydrogen participates in a strong hydrogen bond, and at 3700 cm^{-1} when the –OH is dangling, or unbonded (105). The dangling bonds are also seen in polycrystalline ice films but decrease in population with increasing thickness and are thought to be concentrated at the surface (106). The population is larger in the amorphous thin films (106) and can be reduced in population by irradiation treatment, which allows the initial structure to anneal toward the fully hydrogen-bonded network characteristic of both low-density and high-density amorphous forms (39, 66). The infrared spectroscopy of amorphous water has been studied most intensively by Rice and coworkers (29–30b), and their work is presented in detail in the review of Sceats & Rice (2). The spectra are commonly simplified by studying either the $-$OH stretch when the sample is mostly D_2O or the $-$OD stretch when the sample is mostly H_2O in order to observe the single oscillator frequency, uncoupled from adjacent oscillators of the same frequency.

Somewhat more attention has been given recently to the complimentary Raman spectra (61, 91, 106, 107), partly because they can be obtained from smaller areas of a given sample or from smaller samples (57). The strongest lines in the Raman spectrum come from the $\nu_{\text{dispersive}}$ symmetric stretching modes (61, 91, 106) (3110 cm^{-1} for LDA water and 3200 cm^{-1} for HDA). Kanno et al. (91) stress the similarity of the latter and also the hydrogen-oxygen-hydrogen (HOH) bending component of the Raman spectrum of HDA water to the corresponding bands in the Raman spectrum of aqueous salt solutions.

The internal mode spectroscopy of ASW is dealt with in detail in the work of Sceats & Rice (2), and it would be presumptuous to attempt any summary of it here. In the arena of low-frequency vibrational spectroscopy, however, new and important discoveries have been made (45, 62, 63), which are discussed in the next section.

4.1.2. LOW-FREQUENCY MODES AND IDEAL GLASS CHARACTER OF LDA WATER Contrasting with the individual oscillations of high frequency are the low-frequency collective modes, which in crystals are the well-defined optical and acoustic phonons. These modes are characterized by variable wavelengths. The relation between frequency and wavelength determines, in the case of acoustic modes, the velocity of sound and the elastic moduli. Some extremely interesting and concept-challenging characteristics are found in the case of these modes in amorphous water. Indeed, it is in the behavior of the low-frequency modes and the thermal conductivity that we find evidence that the glassy state of water, in the open-network

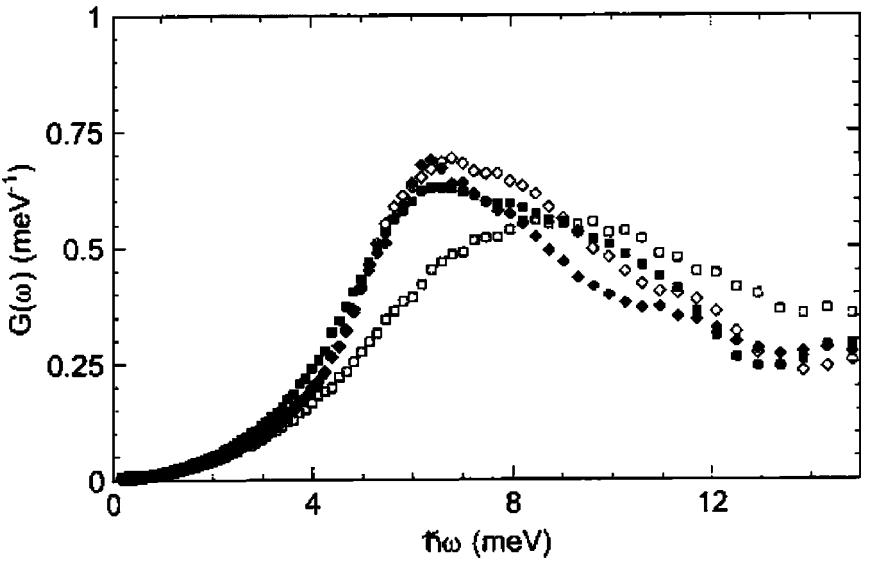

Figure 1 Density of vibrational states of LDA water (symbols), and HDA water compared with those for the crystals ice I_h and ice I_c, showing absence of any boson peak anomaly in the vitreous waters.

low-density form, is of most unusual character among glasses. It may be taken as evidence for the existence of an ideal glass state that is closely approached in the case of glass formation by cooperative de-exitation of the fluid state as in water and liquid silicon cases (108–110a).

Figure 1 shows the low-frequency end of the vibrational frequency density of states (62). In most crystals this region is accurately described by the Debye frequency spectrum, in which the density of states is quadratic in the energy (or frequency, $E = h\nu$). It is broadly believed that, in all glasses, the Debye distribution is unexpectedly violated at low frequencies and long wavelengths where originally it had been expected that the system would behave like a continuum. The breakdown was originally detected by the excess heat capacity found at low temperatures (below 20 K) (111, 111a). It proves to be due to the presence of a group of very low–frequency modes lying in the vicinity of 2–5 meV, or 16–40 cm^{-1}. These modes were detected via an excess light scattering in Raman scattering after correction for the Bose-Einstein population factor and have become known as the Boson peak (112–112b). There is much argument about the precise origin of these modes [reviewed in (113)], though it is generally recognized that they arise from the intrinsic disorder of the glassy state. A review of the findings for the case of water is given in Reference 44. It is seen in Figure 1 that in the case of LDA or HDA water, the excess density of states (DOS) is missing. Vitreous water is indistinguishable

from its crystalline analog, ice I, in this region of the vibrational density of states. It also seems to lack the even lower-energy two-level systems thought to be characteristic of the amorphous solid state (114). Some weak non-Debye features are seen at $\sim$20 cm^{-1} in the study of Klug et al. (114) when the sample temperature increases to 80^1 K, and a molecular dynamics study suggests that these are attributable to a small number of the molecules that exist in special sites considered to be defects (see also Reference 114b). The modes are localized with strong resemblance to those in the soft sphere study of Laird & Schober (114c). Whereas these differences between vitreous waters and other glasses are striking, they are the least astonishing of the low-frequency vibrational mode findings.

More striking is the behavior at short wavelenths. Recently it has become possible to observe phonon excitations at very short wavelengths using inelastic X-ray scattering (115). Because of disorder, it is not expected that the sharp peaks characteristic of crystals could be observed in the case of glasses at short wavelengths. Like all substances, glasses have a well-defined velocity of sound, so the relation between phonon energy and phonon wavelength is precise for long-wavelength low-frequency modes. With most glasses this relationship becomes blurred, that is, the frequency of the energy of a vibration of given wavelength becomes multivalued as shorter wavelengths are examined (meaning that the dispersion relations rapidly broaden with increasing Q value). However, Schober et al. (63) recently reported that, in the case of LDA water, the high Q excitations remain as sharp as for crystals, meaning that well-defined cosine waves exist at all wavelengths in LDA water. For HDA water, the peaks were broader but were still sharp relative to those for most glasses. Figure 2 summarizes these results. Koza (private communication) cautions that the excitations are complex.

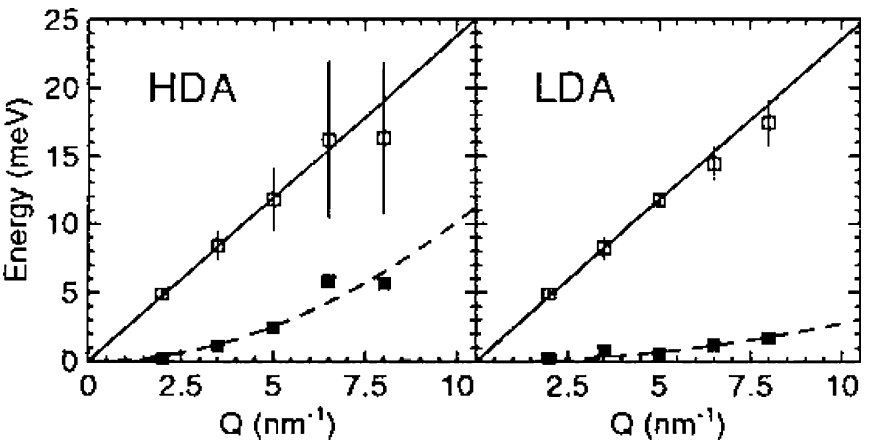

Figure 2 Dispersion relations for HDA and LDA water, determined by inelastic X-ray scattering studies (63). Vertical bars represent the half width of the excitations. Thus, the dispersion curve for LDA water is crystal like.

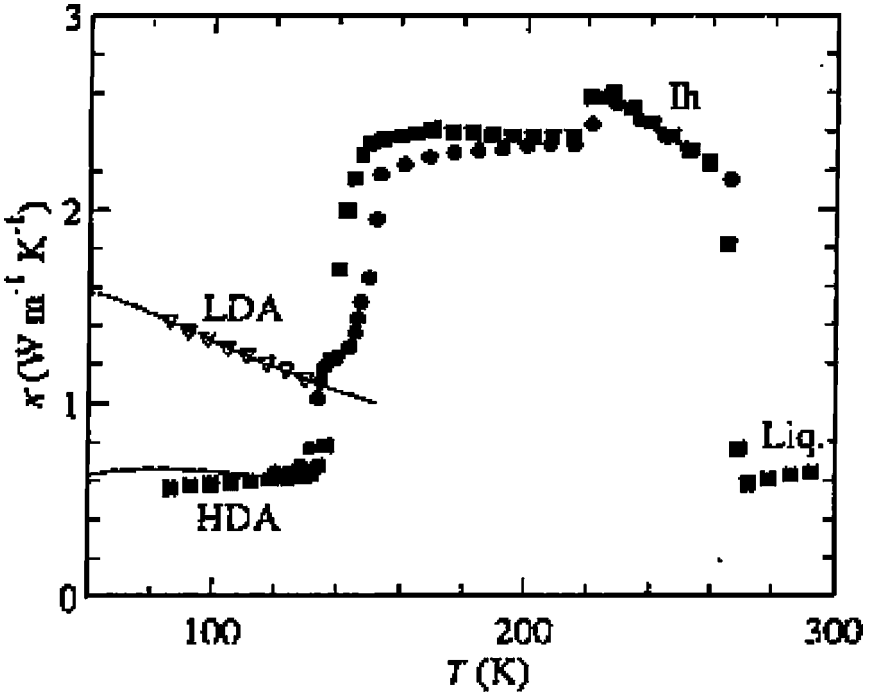

Figure 3 Thermal conductivity versus temperature for two crystalline states of water, ice I_h and ice I_c, and two amorphous states, HDA and LDA. Note the crystal-like increases with decreasing temperature for LDA water.

While the results seen in Figure 2 are astonishing, the most remarkable of all are the recent findings of Andersson & Suga (45) concerning thermal conductivity (shown in Figure 3). These workers have measured the transport of heat through amorphous and crystalline waters using the transient hot wire method. They observed, as expected, that the conductivity decreases suddenly as ice I_h is amorphized under pressure. What is unexpected is that the conductivity increases sharply when HDA water transforms back to LDA. Usually the denser forms of substances are the better thermal conductors. Even more unexpected is that in LDA water the conductivity increases with decreasing temperature, the opposite behavior to that of HDA water and of all other glasses. The LDA behavior is like that of crystals in which the scattering of phonons by other phonons decreases with decreasing sample temperature until finally the limit to the phonon mean free path is set by the sample size. In glasses the phonon mean free path is usually set by the first or second nearest neighbor distance, and the magnitude of the conductivity is determined by phonon population factors.

The finding that the scattering of phonons in a disordered medium can decrease with decreasing temperature, hence that long mean free paths are possible, is novel

and implies the existence of a special kind of order in LDA water. Coupled with the thermodynamic finding that the entropy of ice and LDA water are almost the same (32, 116–117), we are forced to conclude that LDA water is an amorphous solid of a very particular kind, an almost ideal glass, representative of a state of matter somewhere between normal glass and quasi-crystal (110). Even if it can be formed continuously from supercooled water without the first-order liquid-liquid phase transition seen in liquid silicon (108), it probably deserves Speedy's designation of a "new phase of water: Water II" (109). Elsewhere (110, 110a) we have attributed this unusual character to the cooperative manner in which the glass forms from more disordered states (either the liquid or the high-density amorphous forms). It is an embarrassment that, at this time, it is not certain that a characteristic glass transition temperature, T_g, can be assigned to this almost ideal glass.

4.2. Pressure-Volume-Temperature Properties

Because of the similarities of the ASW, HQG, and LDA structures to that of ice I and because of the lack of defect structures to which we have just referred, the pressure-volume-temperature (PVT) properties of these three forms of amorphous water are very similar to those of ice I. Accordingly, one of the peculiarities of ice I is passed on to the low-density forms of amorphous water. This is the occurrence of a negative expansivity domain at low temperatures—a consequence of negative Gruneisen constants for the low-frequency modes that dominate the low-temperature properties. This feature of LDA water (119) disappears with increasing pressure, though most of the change is postponed until the phase transition to HDA water occurs.

The HDA phase displays some anomalous characteristics that are manifested in volumetric as well as thermal measurements (120). However, these have a relaxational character and are discussed in the next two sections.

4.3. Thermal Properties

The thermal properties of amorphous water can be determined by direct calorimetric measurement or by calculation from the density of vibrational states determined by appropriate scattering measurements. The absence of excess low-temperature heat capacity in LDA and HDA water has already been mentioned. From the similarity in vibrational frequency spectra, it can be expected that the heat capacities of low-density glass and ice I will be very similar, as is the case (24).

The enthalpy of the amorphous forms of water become time dependent at higher temperatures as various relaxation processes permit the molecular arrangement to change toward lower enthalpy states. What is observed depends very much on previous thermal history. This behavior is taken up in the next section.

The excess entropy of ASW water over ice I_h is very small (32, 116), considerably smaller than the careful estimate of Sceats & Rice (2). Using a nanoporous glass to prevent crystallization, Oguni and coworkers (120) recently determined the heat capacity of liquid and amorphous water over the entire temperature range

from the melting point down to cryogenic temperatures for a component of the sample that they consider to represent bulk water as opposed to surface water. Based on integration from the fusion point at 273 K, they are able to assess the residual entropy at 0 K and conclude that it is exceptionally low, consistent with the values obtained from evaporation rate measurements at 150 K (32, 117, 118). Indeed, Oguni and colleagues concluded that the residual entropy is less than that of ice I (2.9 J/mol^{-K} versus 3.4 J/mol^{-K}). The relation of this difference to the extent of proton ordering (120) in the two phases is a question of interest.

4.4. Relaxation and Glass Transition

4.4.1. LOW-TEMPERATURE RELAXATIONS Low-temperature relaxations in amorphous water occur whenever the amorphous solid has been prepared far from the conditions in which the relaxation is observed. They appear to be a manifestation of the nonlinearity of relaxation intrinsic to the amorphous state (21, 21a, 124). Hyperquenched water starts to relax during heating at 10 K/min at about 125 K (51b), while HDA water prepared from pressure amorphization of the crystal starts to relax, on comparable timescales, at a lower temperature (∼110 K).

4.4.2. RELAXATIONS RELATED TO THE GLASS TRANSITION Relaxation and the glass transition in the case of amorphous water is a subject of major concern at this time. It has a long and convoluted history that has been reviewed in some detail (12) and is not repeated here. The glass transition, as observed using differntial scanning calorimetry (DSC) at a standard scanning rate, occurs when the enthalpy relaxation time decreases through the value of 100 s. The onset glass transition, T_g, can be assigned using scanning calorimetry or relaxation time data (details in Reference 12).

The general view is that the onset glass transition T_g (12) for vitreous water occurs at about 136 K for ASW and HQG, both on the basis of direct calorimetic determination (26) and by linear extrapolation of unambiguous T_g data from glass-forming binary solutions (12, 25). The directly observed feature is a very weak endotherm, about 14 times weaker than that anticipated by extrapolation from binary solutions, and is only detectable after a special annealing procedure has been carried out. An alternative value of 132 K was recently given by Tulk et al. (61), based on a somewhat different annealing schedule for the HQG. For LDA water the value found is somewhat lower again: 129 K after a 90 min anneal at 127 K (60), or 124 K after annealing at 124–130 K for 2 h and scanning at 10 K/h (59).

A more recent, and conflicting, view (122) is that the extrapolated value of T_g is unreliable due to water network–breaking effects that were ignored in the extrapolation (12) and (123) that the effect directly observed by the anneal-and-scan procedure is an annealing prepeak (124). This prepeak is a shadow of the real glass transition, which is obtained by selecting a portion of the frequency spectrum for the total thermal-relaxation process and enhancing it selectively by the annealing

process. It is characteristic of any system that has moderately nonexponential relaxation character and it is especially enhanced if the sample has initially been rapidly cooled before annealing. Its value depends somewhat on the details of the annealing but usually lies ~10–15% below the real T_g (123, 124).

The shadow T_g is produced in a particularly interesting form during upscan of a stable glass-forming system that has been hyperquenched and then annealed at a temperature well below its actual glass temperature (125–126). The effect, which has striking crossover features in stable glass formers (125, 125a), was seen long ago in the study of certain splat-cooled metallic glasses (126,126a).

This implies that water, above 136 K, is still in the glassy state and remains so until crystallization occurs at 155–160 K. In conflict with this notion are two sets of observations: (*a*) Johari (58b) observed that amorphous water in the LDA form [$T_g = 124$ K at 10 K^{-h} (59) or 129 K at 10 K^{-min} (60)] can be penetrated by a blunt probe at 143 K during scanning at 2 K/min ($\Delta T = 19$ K or 14 K), in apparent qualitative similarity to the fragile glass former *cis*-decalin [$T_g = 137.4$ K at 20 K^{-min} (127) and $T_{(tD=100\ s)} = 134.7$ K (128)], which is penetrated at 140 K (58b). The latter temperature gap is either 2.6 K or 5.3 K, implying in either case that water must be much less fragile than decalin. However, the penetration in LDA water occurs just at the onset of the crystallization process for slow heating [~130 K for 10 K (59) and 155 K for 10 K/min (60)], and the material is said to become much more mobile during crystallization (129). (*b*) Smith & Kay (130) reported that water diffuses like a viscous liquid of very fragile character at 150–155 K. However, they performed these measurements in the temperature range where crystallzation occurs (130), since Avrami coefficients were reported in the range 145–150 K (36). This coincidence also raises questions of reliability.

Some additional input, helpful to the resolution of these conflicts, can be obtained by consideration of the dielectric relaxation measurements that have been made. Data obtained by Johari et al. (37a) on this question are comparable with earlier reports by Skripov and coworkers (37). Both report data as the loss tangent ($\tan\delta = \varepsilon''/\varepsilon'$ where ε'' and ε' are, respectively, the imaginary and real parts of the dielectric constant). We have digitized the $\tan\delta$ data of Johari et al. for an as-prepared (quenched) sample of ASW and in Figure 4 compare them with data for some other well-known glass formers that lack strong secondary relaxations. These are glycerol ($\tan\delta$ data available in Reference 131) and propylene carbonate ($\tan\delta$ data available in Reference 132). We use the familiar scaled temperature presentation T/T_g for the range 0 to 1.40 T_g.

It is seen in Figure 4*a* that the increase in $\tan\delta$, which is rather sudden near T_g for the known glass formers, is slow in the case of water when $T_g = 136$ K is used as the scaling temperature. It is necessary to conclude, as from the penetration measurement, that water is either a very nonfragile liquid near its T_g (133) or it is not a liquid at all.

If we change the scaling temperature to T_g (water) $= 160$ K, then we obtain Figure 4*b*. The data of ASW, glycerol, and PC now overlap up to the crystallization temperature of ASW [~155 K; the highest temperature at which a physical

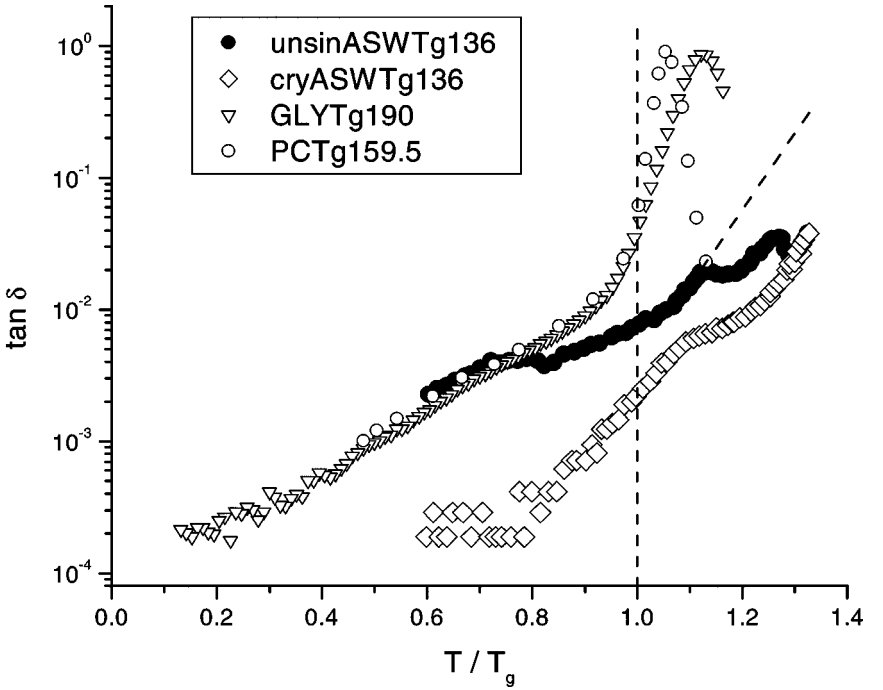

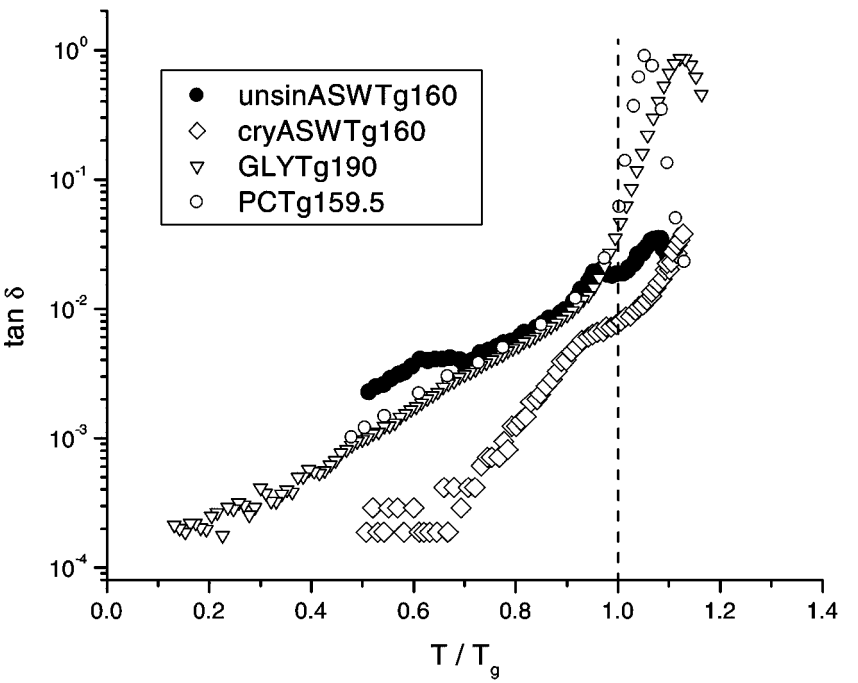

measurement of ASW has ever been made is 160 K (30a, 33, 37)]. Above T_g the data for PC rise more quickly than those for glycerol, in accord with the higher fragility of PC. These data therefore are consistent with the notion that water is not a liquid above 136 K and would be found to be an intermediate or strong liquid above a T_g of about 160 K if it did not crystallize at that temperature. The true situation must remain for future studies to determine. New diffusivity-measuring techniques now under development (B.D. Kay, private communication; M.D. Ediger, private communication) should shortly be able to confirm (or deny) that the diffusivity of water remains low and glass like up to 150 K.

It should be possible to observe the shadow transition in the high density–water glasses produced by the high-pressure liquid-cooling procedures[1] of Mishima & Suzuki (52) or of the electron microscopists (53–53b). The shadow T_g in this case should lie at a lower temperature than in HQG, ASW, or LDA water because HDA water is not an open network (but all annealing and scanning would have to be carried out at high pressure!). The properties of glasses quenched under controlled pressure in the vicinity of 0.2 GPa would be particularly interesting to observe because it is possible they could show two shadow T_g s due to two different glasses (polyamorphic forms) being present. The polyamorphism of water provides the material for the next section.

[1]It should be relatively easy to obtain the glassy state of water at 0.2 GPa, because the homogeneous nucleation temperature is depressed down to -90°C (133a). I once plunged a 50-micron glass capillary containing 2 cm of water under oil-transmitted pressure of 0.2 GPa into liquid nitrogen and observed it to remain unchanged in appearance or length, which implies vitrification. Unfortunately, after the crystallization that occurred during warm-up (when the length indeed changed), the observation could never be repeated, because the sample always crystallized (the mysterious crystal memory effect). In view of the present controversy about the T_g of water, more experimental studies of glass formation and transition under pressure will be important to conduct.

Figure 4 (a) The dielectric relaxation (represented by $\tan\delta = \varepsilon''/\varepsilon'$) of amorphous water ASW films [results of Johari et al. (37a)] compared with those for two other high dielectric constant liquids that do not crystallize. The dashed line indicates the (unobservable) extension of the water data above its crystallization temperature near 155 K. The data are compared by plotting as function of T/T_g, using $T_g = 136$ K for water. If indeed $T_g = 136$ K then water must be an extremely strong liquid, relative to the other two, whose rates of increase near T_g are in the order of their fragilities. T_g values are indicated in the legend. Glycerol is intermediate in the strong-fragile classification (21). (b) The same data, replotted with T_g for water set at 160 K. Now the water data coincide with those of propylene carbonate (PC) and slightly exceed those of glycerol, up to the ASW crystallization point. The low-temperature excess tan δ for water is evidently (37a) a consequence of the high fictive temperature and largely disappears on sintering (37a).

It is also possible to observe shadow glass transitions in aqueous solutions (134) and extrapolate them to meet the pure water value. Hofer et al. (134) discussed the difficulty of separating the effects they reported as T_g values, from the annealing prepeaks discussed by other authors. I now believe they were all pre-peaks, i.e., "shadow" T_g s. With the combination of pressure, solutes, and small sample techniques as additional variables, some experimental resolution of the glass transition problem for water should be attainable in the near future.

5. POLYAMORPHISM

The phenomenon of polyamorphism is now attracting a lot of attention. Confusion abounds concerning what is to be viewed as a polyamorphic change in a system (12a). Water seems to provide one of the few clear examples of the phenomenon, though so far even this case has not been able to provide a direct example of a thermodynamically reversible transition. The only case where an equilibrium phenomenon has been observed (i.e., two equilibrated phases of different amorphous structures in coexistence) is that of phosphorus (135), and this is more correctly seen as a vapor-liquid equilibrium since one of the phases is above its critical temperature. A good introduction to the thermodynamic aspects of polyamorphism is provided in a recent article by McMillan (136).

The conditions under which at least two distinct density states of HDA and LDA water can be produced are described in Section 2, with mention made of the abrupt change from one form to the other. In this section we look at the phenomenon of polyamorphic change in amorphous water in more detail.

The relationship between crystalline polymorphs can be represented on a phase equilibrium diagram. There is a precise temperature and pressure at which the free energies of the two phases are equal and on either side of which one phase or the other is metastable. The growth of one polymorph from the other by transport across a phase boundary can usually be observed. This is rarely the case with amorphous materials. However, the phase boundary and its movement have been observed in the case of amorphous water (137) and this is perhaps the strongest reason for believing that the pressure-induced density crossover in amorphous water is a true polyamorphic change. It is disturbing that it cannot be seen to occur reversibly at 140 K, where the liquid is supposed to be internally equilibrated for timescales of minutes (if T_g is 136 K), but this could simply be a reflection of the mis-assignment of T_g discussed in the previous section.

The kinetics of the process have recently been subject to detailed study. Stal'gorova et al. (65, 65a) and Lyapin et al. (65b) used ultrasonics to observe a (spinodal-like) softening that precedes the phase change in either direction. Koza et al. (64) conducted quantitative analysis of the evolution of the static structure factor obtained from neutron scattering studies and concluded that the conversion of HDA water to LDA proceeds in three stages. The first stage is a relaxation of the high-density phase to lower densities in the normal manner of glassy relaxation

from some high-energy state. Performed in a series of isothermal steps, this can be mistaken for the sampling of "several distinct metastable forms" (61a), due to the logarithmic approach to equilibrium at a given temperature. As with any glass, there are effectively an infinite number of distinct states, depending on time-temperature history, but these all belong to the same polyamorph (configuration space) megabasin (139) until the second stage of the process begins. The second stage is the polyamorphic transformation to LDA water, during which the spectra change in a manner that can be accounted for by linear addition of two distinct components. A third and final stage follows the completion of the transformation when the LDA water, now in its own megabasin, further relaxes toward the equilibriated LDA form. The initial relaxation is faster and the final equilibration more complete, the higher the temperature of observation.

The two-state process is well accounted for using the Avrami-Kolmorogorov phase transformation kinetic equations (64). Because the system is observed in a state far from equilibrium, all molecular displacement processes occur on short timescales relative to the timescales on which they would occur in the equilibrium state. This is a manifestation of the nonlinearity of relaxation processes in amorphous materials (21, 124), and is qualitatively interpreted using a Scherer-Hodge kinetic model (124) based on the Adam-Gibbs model (140). This model is semiquantitive for relaxation processes not far from equilibrium, but it apparently breaks down seriously under far-from-equilibrium conditions (141).

The phase transformation process has been attractive to computer modelers and theorists (142–145). Tse & Klein (142) made the first attempt to simulate it. Poole et al. have studied it by molecular dynamics (MD) (8, 8a) in both ST2 and TIP-4P potentials and found it a much bolder phenomenon in the former. They suggested that the transition was closely related to a critical point in the supercooled liquid phase for which they produced the first evidence. It has also been examined in the SPC-E potential by Giovambattista et al. (144), who applied a potential energy landscape approach and showed that the system (not too surprisingly) did not follow a path that would be explored under equilibrium conditions. They concluded that observations on the glass-glass transition could not be directly related to the liquid-state phenomena. A similar point was made by Tse et al. (55), who argued that the spinodal collapse was accomplished by filling the holes in the ice I_h structure with interstitials. They believed this retained the crystal structure information in a microcrystalline manner and that this was not therefore directly related to the structure of the liquid. As mentioned above, Finney et al. (44a) contradict this view.

Sasai (145) has used computer simulations as both inspiration for and a source of data for the testing of simple order–parameter models for the polyamorphic transition. Ponyatovsky and coworkers (146) tried to adapt a two-liquid (one order parameter) model to describe the water behavior but were derailed by analytic errors (C.T. Moynihan, private communication). Moynihan (147) applied a similar model, using the observed limits of compression and decompression as spinodal boundaries to fix parameters in the model, with some apparent success. Tanaka (148, 148a) has described a two-order parameter (bond distance and bond

orientation) model to describe the conversion, and a geometrical approach to the definition of such order parameters has been given by Errington & Debenedetti (149), who used it to analyze the liquid behavior. All of these bear fundamentally on the question of whether there is a liquid-liquid transition, terminated by a critical point within the supercooled liquid state of water (8, 8a, 150), but this fascinating possibility has deliberately been set outside the scope of this review. Interested readers will find the current state of play well summarized in References 12b, 150, and 151. Additional considerations of interest bearing on the possibility of multiple critical points (hence on the additional polyamorphic forms envisioned by Rice and coworkers (2), may be found in Reference 102.

ACKNOWLEDGMENTS

This work has been supported by the NSF under Solid State Chemistry Grant No. DMR-00,82535. We are grateful to Ayumi Minoguchi and Ranko Richert for assistance with Figure 4.

The *Annual Review of Physical Chemistry* is online at http://physchem.annualreviews.org

LITERATURE CITED

1. Angell CA. 1983. *Annu. Rev. Phys. Chem.* 34:593–630
2. Sceats MG, Rice SA. 1982. In *Water: A Comprehensive Treatise*, ed. F Franks, pp. 83–211. London: Plenum
3. Burton EF, Oliver WF. 1935. *Nature* 135:505
3a. Burton EF, Oliver WF. 1935. *Proc. R. Soc. London Ser. A* 153:166
4. Jenniskens P, Blake DF. 1994. *Science* 265:753
4a. Jenniskens P, Barnhak SF, Blake DF, McCoustra MRS. 1997. *J. Chem. Phys.* 107:1232
5. Mishima O, Calvert LD, Whalley E. 1984. *Nature* 310:393–95
5a. Mishima O, Calvert LD, Whalley E. 1985. *Nature* 314:76
5b. Klug DD, Mishima O, Whalley E. 1987. *J. Chem. Phys.* 86:5323
6. Mishima O, Takemure K, Aoki K. 1991. *Science* 254:406
7. Mishima O. 1994. *J. Chem. Phys.* 100:5910
8. Poole PH, Sciortino F, Essmann U, Stanley HE. 1992. *Nature* 360:324
8a. Poole PH, Sciortino F, Essmann U, Stanley HE. 1993. *Phys. Rev. E* 48:4605
9. Poole PH, Sciortino F, Grande T, Stanley HE, Angell CA. 1994. *Phys. Rev. Lett.* 73:1632–35
10. Angell CA, Sare E. 1970. *J. Chem. Phys.* 52:1058
10a. Angell CA, Sare E. 1968. *J. Chem. Phys.* 49:4713
11. Wolf GH, Wang S, Herbst CA, Durben DJ, Oliver WJ, et al. 1992. In *High-Pressure Research: Application to Earth and Planetary Sciences*, ed. YS Manghnani, MH Manghnani. Tokyo/Washington: Terra Sci./Am. Geophys. Union
12. Angell CA. 2002. *Chem. Rev.* 102: 2627
12a. Yarger JL, Angell CA. 2003. *Chem. Rev.* In press
12b. Debenedetti PG. 2003. *J. Phys. Condens. Matter* 15:R1669–726

13. Hancock BC, Shalaev EY, Shamblin SL. 2002. *J. Pharm. Pharmacol.* 54:1151–52
14. Yarger JL, Angell CA, Borick SS, Wolf GH. 1997. In *Supercooled Liquids: Advances and Novel Applications*, ed. J Fourkas, D Kivelson, U Mohanty, K Nelson, *ACS Symp. Ser.* 676. Washington, DC: Am. Chem. Soc.
15. McNeil LE, Grimsditch M. 1992. *Phys. Rev. Lett.* 68:83
16. Polsky CH, Smith KH, Wolf GH. 1999. *J. Non-Cryst. Solids* 248:159–68
17. Polsky CH, Martinez LM, Leinenweber K, VerHelst MA, Angell CA, Wolf GH. 2000. *Phys. Rev. B* 61:5934–38
18. El'kin FS, Brazhkin VV, Khvostantsev LG, Tsiok OB, Lyapin AG. 2002. *JETP Lett.* 75:342–47
19. Tsiok OB, Brazhkin VV, Lyapin AG, Khvostantsev LG. 1998. *Phys. Rev. Lett.* 80:999–1002
20. Woodcock LV, Angell CA, Cheeseman PA. 1976. *J. Chem. Phys.* 65:1565
20a. Boulard B, Angell CA, Kieffer J, Phifer CC. 1992. *J. Non-Cryst. Solids* 140:350–58
20b. Shao J. 1993. *Chin. Phys. Lett.* 10:669
20c. Lacks DJ. 2000. *Phys. Rev. Lett.* 84:4629
21. Angell CA. 1995. *Science* 267:1924
21a. Angell CA, Poole PH, Shao J. 1994. *Nuovo Cimento D* 16:993
22. Ghormley JA. 1967. *J. Chem. Phys.* 48:503
23. McMillan JA, Los SC. 1965. *J. Chem. Phys.* 42:829
24. Sugisaki M, Suga S, Seki S. 1968. *J. Chem. Soc. Jpn.* 41:2591
25. MacFarlane DR, Angell CA. 1984. *J. Phys. Chem.* 88:759
26. Johari GP, Hallbrucker A, Mayer E. 1987. *Nature* 330:552–53
27. Hallbrucker A, Mayer E, Johari GP. 1989. *Philos. Mag.* 60:179
27a. Hallbrucker A, Mayer E, Johari GP. 1989. *J. Phys. Chem.* 93:7551
27b. Mayer E, Hallbrucker A, Sartor G, Johari GP. 1995. *J. Phys. Chem.* 99:5161–65
28. Buentempo V. 1972. *Phys. Lett. Ser. A* 42:17
29. Olander DS, Rice SA. 1972. *Proc. Natl. Acad. Sci. USA* 69:98
29a. Rice SA. 1975. *Top. Curr. Chem.* 60:109
30. Sivakumar TC, Rice SA, Sceats MG. 1978. *J. Chem. Phys.* 69:3468
30a. Rice SA, Bergren M, Swingle L. 1978. *Chem. Phys. Lett.* 59:14
30b. Sceats MG, Rice SA. 1979. *J. Chem. Phys.* 71:793
31. Yoshimura Y, Kanno H. 2001. *Chem. Phys. Lett.* 349:51–56
32. Speedy RJ, Debenedetti PG, Smith RS, Huang C, Kay BD. 1996. *J. Chem. Phys.* 105:240
33. Koverda VP, Bogdanov NM, Skripov VP. 1983. *J. Non-Cryst. Solids* 57:203
34. Schmitt B, Grim SRJA, Greenberg J, Klinger J. 1992. In *Proc. VIIIth Symp. Phys. Chem. Ice*, ed. N Maeno, T Hondoh, p. 344. Sapporo, Jpn: Hokkaido Univ. Press
35. Jenniskens P, Blake DF. 1996. *Astrophys. J.* 473:1104
36. Smith RS, Huang C, Wong EKL, Kay BD. 1996. *Surf. Sci. Lett.* 367:L13
37. Koverda VP, Skokov VW, Faizillin MZ, Bogdanov NM, Skripov VP. 1977. *Russ. J. Phys. Chem. Glasses* 3:186
37a. Johari GP, Hallbrucker A, Mayer E. 1991. *J. Chem. Phys.* 95:2955
38. Wenzel J, Linderstrom CU, Rice SA. 1975. *Science* 187:428
39. Narten AH, Venkatesh CG, Rice JA. 1976. *J. Chem. Phys.* 64:1106
40. Scott RS, Kay BD. 1999. *Nature* 398:788
40a. Smith RS, Huang C, Kay BD. 1997. *J. Phys. Chem.* 101:6123
41. Tsekouras AA, Iedema MJ, Cowin JP. 1998. *Phys. Rev. Lett.* 80:5798
42. Dubochet J, Lepault EM. 1984. *J. Phys.* 9:C7–85
43. Kolesnikov AI, Li JC, Parker SF, Eccleston RS, Loong C-K. 1999. *Phys. Rev. B* 59:3569
43a. Li JC, Kolesnikov AI. 2002. *J. Mol. Liq.* 100:1

44. Yamamuro O, Madokoro Y, Yamasaki H, Matsuo T. 2001. *J. Chem. Phys.* 115:9808
44a. Finney JL, Bowron DT, Soper AK, Loerting T, Mayer E, Hallbrucker A. 2002. *Phys. Rev. Lett.* 89:205503
45. Andersson O, Suga H. 2002. *Phys. Rev. B* 65:140201
46. Brüggeller P, Mayer E. 1980. *Nature* 288:569
46a. Brüggeller P, Mayer E. 1982. *Nature* 298:715
47. Dubochet J, McDowell AW. 1981. *J. Microsc.* 124:RP3
48. Mayer E. 1985. *J. Appl. Phys.* 58:663
48a. Mayer E. 1985. *J. Microsc.* 140:3
48b. Mayer E. 1986. *J. Microsc.* 141:269
49. Hayes JM, Reinot T, Shields P, Small GJ. 1999. *Rev. Sci. Instr.* 70:2454–57
49a. Reinot T, Dang NC, Small GJ. 2002. *J. Lumin.* 98:183–88
50. Brower WE, Schedgick DJ, Bigelow LK. 2002. *J. Phys. Chem. B* 106:4565
51. Johari GP, Hallbrucker A, Mayer E. 1987. *Nature* 330:552
51a. Hallbrucker A, Mayer E, Johari GP. 1989. *Philos. Mag. B* 60:179
51b. Hallbrucker A, Mayer E. 1987. *J. Phys. Chem.* 91:503
51c. Fleissner G, Hallbrucker A, Mayer E. 1998. *J. Phys. Chem. B* 102:6239
51d. Hage W, Hallbrucker A, Mayer E, Johari GP. 1994. *J. Chem. Phys.* 100:2743
51e. Hage W, Hallbrucker A, Mayer E, Johari GP. 1995. *J. Chem. Phys.* 103:545
52. Mishima O, Suzuki Y. 2001. *J. Chem. Phys.* 115:4199
53. Sartori N, Richter K, Dubochet J. 1993. *J. Microsc.* 172:55
53a. Moor H, Riehle U. 1968. *Micron* 2:33
53b. Moor H. 1987. In *Theory and Practice of High Pressure Freezing Cryotechniques in Biological Electron Microscopy*, ed. RA Steinbrecht, K Zierold, pp. 175–91. Berlin: Springer-Verlag
54. Bingelli N, Chelikovsky JR. 1992. *Phys. Rev. Lett.* 69:2220
54a. Sciortino F, Essman U, Stanley HE, Hemmati M, Shao J, et al. 1995. *Phys. Rev. E* 52:6484
55. Tse JS, Klug DD, Tulk CA, Swainson EC, Svennson C-K, et al. 1999. *Nature* 400:647
56. Floriano MA, Whalley E, Svensson EC, Sears VF. 1986. *Phys. Rev. Lett.* 57:3062–64
57. Mishima O, Suzuki Y. 2002. *Nature* 419:599
58. Johari GP. 2000. *J. Chem. Phys.* 112:8573; 113:10412
58a. Johari GP. 1998. *J. Phys. Chem. B* 102:4711
58b. Johari GP. 2000. *Phys. Chem. Chem. Phys.* 2:1567
59. Handa YP, Klug DD. 1988. *J. Phys. Chem.* 92:3323
60. Johari GP, Hallbrucker E, Mayer E. 1996. *Science* 273:90–92
61. Tulk CA, Klug DD, Branderhorst R, Sharpe P, Ripmeester JA. 1998. *J. Chem. Phys.* 109:8478
61a. Tulk CA, Benmore CJ, Urquidi J, Egelstaff PA, Klugg DD, et al. 2002. *Science* 297:1320–23
62. Schober H, Koza M, Tölle A, Fujara F, Angell CA, Bohmer R. 1998. *Physica B* 241–243:897–902
63. Schober H, Koza MM, Tölle A, Masciovecchio C, Sette F, et al. 2000. *Phys. Rev. Lett.* 85:4100
64. Koza MM, Schober H, Fischer HE, Hansen T, Fujara F. 2003. *J. Phys. Condens. Matter* 13:321
65. Stal'gorova O, Grommitskaya EL, Brazhkin VV, Lyapin AG. 1999. *Pis'ma Zh. Eksp.Teor. Fiz.* 69:653
65a. Stal'gorova O, Grommitskaya EL, Brazhkin VV, Lyapin AG. 1999. *JETP Lett.* 69:694 (Engl. version)
65b. Lyapin AG, Brazhkin VV, Grommitskaya EL, Mukhamadiarov VV, Stal'gorova OV, Tsiok OB. 2002. See Ref. 152, pp. 449–68
66. Hallbrucker JL, Kohl A, Soper AK, Bowron DT. 2002. *Phys. Rev. Lett.* 88: 225503

67. Sartori N, Bednar J, Dubochet J. 1996. *J. Microsc.* 182:163
68. Al-Amoudi A, Dubochet J, Studer D. 2002. *J. Microsc.* 207:146
69. Dubochet J, LePault J, Freeman R, Berriman JA, Homo JC. 1982. *J. Microsc. Oxford* 128:219
70. Chiu W. 1986. *Annu. Rev. Biophys. Chem.* 15:237
71. Gabashvili IS, Agrawal RK, Spahn CMT, Grassucci RA, Svergun DI, et al. 2000. *Cell* 100:537
72. Hud NV, Downing KH. 2001. *Proc. Natl. Acad. Sci.USA* 98:14925–30
73. Jeanloz R. 1984. *EOS* 65:1245
74. Tulk CA, Klug DD. 2001. *Phys. Rev. B* 63:212201
75. Bogardus AE, Roy RS. 1965. *J. Am. Ceram. Soc.* 48:205
75a. Ermakov AE, Yurchikov EE, Bariniov VA. 1981. *Fiz. Metal. Metalloved.* 54:1184
75b. Yamamuro O, Tsukushi I, Matsuo T. 1996. *Mol. Cryst. Liq. Cryst.* 276:A205–14
76. Heide HG. 1984. *Ultramicroscopy* 14:271
76a. Strazzula G, Baratta GA, Leto G, Foti G. 1992. *Europhys. Lett.* 18:517
77. Heide HG, Zeitler E. 1984. *Ultramicroscopy* 16:151
77a. Kouchi A, Kuroda T. 1990. *Nature* 344:134
78. Matsumoto M, Saito S, Ohmine I. 2002. *Nature* 416(6879):409
79. Yamada M, Mossa S, Stanley HE, Sciortino F. 2002. *Phys. Rev. Lett.* 88:195701
80. Giovambattista N, Angell CA, Stanley HE, Sciortino F. 2004. *Phys. Rev. Lett.* Submitted
81. Tombari E, Ferrari C, Salvetti G. 1999. *Chem. Phys. Lett.* 300:749–51
82. Angell CA. 2001. In *Water Science for Food, Health, Agriculture and Environment*, ed. Z Berk, RB Leslie, PJ Lilford, S Mizrahi, pp. 1–30. Lancaster: Technomic ISOPOW 8
83. Deleted in proof
84. Bizid A, Bosio L, Defrain A, Oumezzine M. 1987. *J. Chem. Phys.* 87:2225
85. Bellissent-Funel MC, Teixeira J, Bosio L. 1987. *J. Chem Phys.* 87:2231–35
86. Chowdury MR, Dore JC, Wenzel JT. 1982. *J. Non-Cryst. Solids* 53:247
87. Dore JC. 1990. *J. Mol. Struct.* 237:221
88. Bellissent-Funel MC, Bosio L, Hallbrucker E, Mayer E, Sridi-Dorbez R. 1992. *J. Chem. Phys.* 97:1282
89. Hallbrucker A, Mayer E, O'Mard LP, Dore JC, Chieux P. 1991. *Phys. Lett. A* 159:406
90. Floriano MA, Handa YP, Klug DD, Whalley W. 1989. *J. Chem. Phys.* 91:7187–92
91. Kanno K, Tomikawa K, Mishima O. 1998. *Chem. Phys. Lett.* 293:412
91a. Yoshimura Y, Kanno H. 2001. *Chem. Phys. Lett.* 349:51–56
92. Dubochet J, Richter K, Roy HV, McDowall AW. 1991. *Scan. Micros.* 5(4):S11–16
93. Koza M, Schober H, Tölle A, Fujara F, Hansen T. 1999. *Nature* 397:660
94. Kohl I, Mayer E, Hallbrucker A. 2001. *Phys. Chem. Chem. Phys.* 3:602
95. Lobban C, Finney JL, Kuhs WF. 1998. *Nature* 391:268
96. O'Keeffe M. 1998. *Nature* 392:879
97. Mishima O, Calvert LD, Whalley E. 1984. *Nature* 314:76
98. Johari G. 2000. *J. Chem. Phys.* 112:1
99. Loerting T, Salzmann C, Kohl I, Mayer E, Hallbrucker A. 2001. *Phys. Chem. Chem. Phys.* 3:5355–57
100. Klotz S, Hamel G, Loveday JS, Nelmes RJ, Guthrie M, Soper AK. 2002. *Phys. Rev. Lett.* 89:285502
101. Deleted in proof
102. Brovchenko I, Geiger A, Oleinikova A. 2003. *J. Chem. Phys.* 118:9473–76
103. Klug DD. 2002. *Nature* 420:749
104. Angell CA. 1997. *Physica D* 107:122–42
105. Palumbo ME, Strazzulla G. 2003. *Can. J. Phys.* 81:217–24

106. Mitlin S, Leung KT. 2002. *J. Phys. Chem. B* 106:6234–47
107. Mitterbock M, Fleissner G, Hallbrucker A, Mayer E. 1999. *J. Phys. Chem. B* 103:8016
108. Sastry S, Angell CA. 2003. *Nature* 2:739–43
109. Speedy RJ. 1992. *J. Phys. Chem.* 96:2322
110. Angell CA. 2000. *Solid State Sci.* 2:791–805
110a. Angell CA, Moynihan CT, Hemmati M. 2000. *J. Non-Cryst. Solids* 274:319–31
111. Zeller RC, Pohl RO. 1971. *Phys. Rev. B* 4:2029
111a. Pohl RO. 1981. In *Amorphous Solids: Low Temperature Properties*, ed. WA Phillips, p. 27. Berlin/Heidelberg/New York: Springer-Verlag
112. Malinovsky VK, Sokolov AP. 1986. *Solid State Commun.* 57:757
112a. Malinovsky VK, Novikov VN, Parshin PP, Sokolov AP, Zemlyanov MG. 1990. *Europhys. Lett.* 11:43
112b. Duval E, Boukanter A, Achibat T. 1990. *J. Phys. Condens. Matter* 2:10227
113. Angell CA, Ngai KL, McKenna GB, McMillan PF, Martin SW. 2000. *J. Appl. Phys.* 88:3113–57
114. Klug DD, Tse JS, Shpakov V, Tulk CA, Swainson I, et al. 2002. See Ref. 152, pp. 391–402
114a. Agladze NI, Sievers A. 1998. *J. Phys. Rev. Lett.* 80:4209
114b. Angell CA, Yue Y-Z, Wang LM, Copley JRD, Borick S, Mossa S. 2003. *J. Phys. Condens. Matter* 15:S1051–68
114c. Laird BR, Schober HR. 1991. *Phys. Rev. Lett.* 66:636
115. Sette F, Ruocco G, Krisch M, Bergmann U, Masciovecchio C, et al. 1995. *Phys. Rev. Lett.* 75:850
116. Whalley E, Klug DD, Handa YP, Svensson EC, Root JH, Sears VF. 1991. *J. Mol. Struct.* 250:337
117. Kouchi A. 1987. *Nature* 330:550
118. Lofgren P, Ahlstrom P, Lausma J, Kasemo B, Chakarov D. 2003. *Langmuir* 19:265–74
119. Tanaka H. 2001. *J. Mol. Liq.* 90:323
120. Maruyama S, Wakabayashi K, Oguni M. 2004. *Phys. Rev. Lett.* In press
121. Tajima Y, Matsuo T, Suga H. 1996. *Nature* 299:810
122. Velikov V, Borick S, Angell CA. 2001. *Science* 294:2335–38
123. Yue Y-Z, Angell CA. 2004. *Nature.* In press
124. Hodge IM. 1994. *J. Non-Cryst. Solids* 169:211–66
125. Yue Y-Z, Christiansen J de C, Jensen SL. 2002. *Chem. Phys. Lett.* 357:20
125a. Yue Y-Z, Christiansen J de C, Jensen SL. 2002. *Appl. Phys. Lett.* 81:2983–85
126. Chen HS, Inoue A. 1984. *J. Non-Cryst. Solids* 61–62:805–9
126a. Inoue A, Matsumoto T, Chen HA. 1985. *J. Mater. Sci.* 20:4057–68
127. Wang L-M, Velikov V, Angell CA. 2002. *J. Chem Phys.* 117:10191
128. Duvurri K, Richert R. 2002. *J. Chem. Phys.* 117:4414
129. Koverda VP, Bogdanov NM, Skripov VP. 1983. *J. Non-Cryst. Solids* 57(2):203–12
130. Smith RS, Kay BD. 1999. *Nature* 398:788–91
131. Hansen C, Richert R. 1997. *J. Phys. Condens. Matter* 9:9961–71
132. Johari GP, Goldstein M. 1970. *J. Chem. Phys.* 53:2372
133. Ito K, Moynihan CT, Angell CA. 1999. *Nature* 398:492
133a. Kanno H, Speedy RJ, Angell CA. 1975. *Science* 189:880
134. Hofer K, Hallbrucker A, Mayer E, Johari GP. 1989. *J. Phys. Chem.* 93:4674–77
135. Katayama Y, Mizutani T, Utsumi W, Shinomura O, Yamakata M, Funakoshi K. 2000. *Nature* 403:170–73
136. McMillan PF. 2002. *Proc. Int. School of Physics, "Enrico Fermi" Course CXLVII*, ed. RJ Hemley, GL Chiarotti, M Bernasconi, L Ulivi. Amsterdam: IOS Press

137. Mishima O. 1991. *Science* 254:406
138. Deleted in proof
139. Angell CA. 1997. *Phys. D* 107:122–42
140. Adam G, Gibbs JH. 1965. *J. Chem. Phys.* 43:139
141. Huang J, Gupta P. 1992. *J. Non-Cryst. Solids* 151:175
142. Tse JS, Klein M. 1987. *Phys. Rev. Lett.* 58:1672
143. Saitta AM, Datchi F. 2003. *Phys. Rev. E* 67:020201
144. Giovambattista N, Stanley HE, Sciortino F. 2003. *Phys. Rev. Lett.* 91:115504
145. Sasai M. 2000. *Physica A* 285:315
146. Ponyatovsky EG, Sinitsyn VV, Pozdnyakova TA. 1994. *JETP Lett.* 60:360
147. Moynihan CT. 1997. *Mater. Res. Soc. Symp.* 455:411
148. Tanaka H. 1999. *J. Phys. Condens. Matter* 11:L159
148a. Tanaka HJ. 2000. *Chem. Phys.* 112:799
149. Errington JR, Debenedetti PG. 2001. *Nature* 409:318
150. Mishima O, Stanley HE. 1998. *Nature* 396:329
151. Debenedetti PG, Stanley HE. 2003. *Phys. Today* 15:R1669–736
152. Brazhkin VV, Buldyrev SV, Ryzhov VN, Stanley HE, eds. 2002. *New Kinds of Phase Transition: Transformations in Disordered Substances.* Dordrecht: Kluwer Acad.

Annual Review of Physical Chemistry
Volume 55, 2004

CONTENTS